Research article

Journal of RAMAN SPECTROSCOPY

Received: 8 June 2013 Revised: 14 December 2013 Accepted: 15 December 2013 Published online in Wiley Online Library: 28 January 2014

(wileyonlinelibrary.com) DOI 10.1002/jrs.4447

Micro-analysis on Chinese over-glaze red decoration of Linshui Kiln from Jin dynasty (1115–1234 AD)

Wentao Hao,[a,b] Wugan Luo,[a,b] Yue Chen[a,b]* and Changsui Wang[a,b]

Red and green over-glaze decoration on Chinese porcelains from the Song-Jin periods is critical to the development for Chinese ceramics. To characterize the identity, crystal size, and band gap width of the red colorant, red and green porcelain shards from the Linshui kiln produced in the Jin dynasty (1115–1234 AD) are investigated using Raman spectroscopy, X-ray diffractometry, and diffuse reflectance measurements. The colorant is shown to comprise hematite crystallites with the average diameter around 30 nm, and its crystal lattice is distorted as the result of the low firing of the decoration. The use of crystal size estimations coupled with band gap width calculations are believed to be employed for the first time on the study of Chinese archeological artifacts. Copyright © 2014 John Wiley & Sons, Ltd.

Additional supporting information may be found in the online version of this article at the publisher's web site.

Keywords: over-glaze decoration; red colorant; hematite crystallites; distorted lattice structure

Introduction

Chinese red and green porcelain (*Honglvcai*) first emerged during Song-Jin Periods (960–1234 AD), and the decorations attached on their glaze surface are generally in red, green, and/or yellow color.[1] Among all colors, the red one is particularly significant. By literature, the raw material of red over-glaze decoration is the mixture of lead-contained minerals and hematite, which is obtained from melanterite ($FeSO_4 \times 7H_2O$) by heating, grinding, washing, and drying. After smearing (drawing) on the surface of white glaze, the so-called vitriolum red (*Fanhong*) as the red pigment began to be formed during the low firing process in the kiln at temperature around 800 °C.[1,2]

It is widely believed that *Honglvcai* was first successfully invented at *Cizhou* kiln.[1] Long before the emergence of *Honglvcai*, craftsmen in this area began to fire painted potteries during prehistoric period.[3] In Sui-Tang periods (581–907 AD), white porcelain started to be fired here together with black porcelain, celadon, and low-fired *Sancai*.[4] Then from Song to Jin dynasty (960–1234 AD), other inventions arose such as black and/or brown under-glaze decorations combined with red and green over-glaze decorations. During Song-Jin periods (960–1234 AD), porcelain production in *Cizhou* district gradually peaked, and the well-known '*Cizhou* kiln system' formed.[1] Among all individual kilns in *Cizhou* kiln system, *Linshui* kiln is especially significant because of its early emergence dating to Sui-Tang periods (581–907 AD) and its great influence on adjacent kilns, such as Guantai kiln and Pengcheng kiln.[5]

Since the significant status of *Cizhou* kiln system, a thorough study on its products is meaningful and necessary. However, scientific researches in this field are quite few. Previous studies on Chinese porcelains were typically focused on analyses of elemental compositions[6–9] and valence states.[10,11] In this paper, investigations on crystal sizes and band gap widths of red colorants were carried out on several *Honglvcai* shards of Jin dynasty (1115–1234 AD) from Linshui kiln of Hebei province by Raman spectroscopy analysis, X-ray diffraction (XRD), and ground state diffuse reflectance measurements. This is probably the first application of crystal size estimation and band gap width calculation on the archeological porcelains.

Experimental

Samples/sampling

All samples were excavated from Linshui kiln site in Hebei Province dating to Jin dynasty (Fig. S1). From May to June of 2002, Heritage Management Sector of Handan implemented a rescue excavation in the third coal mine district of Linshui. In this site, one ceramics kiln, ten kiln basins, and one *Honglvcai* workshop were found, together with large amount of kiln furniture facilities and porcelain shards covered by green glaze, yellow glaze, white engobed glaze, *Honglvcai*, black under-glaze decorations, and so on. A total of five *Honglvcai* shards with red decorations on the glaze were analyzed here, and their numbers are a-3, a-4, a-5, b-9, and b-16 (Fig. S2).

* *Correspondence to: Yue Chen, Key Laboratory of Vertebrate Evolution and Human Origins of Chinese Academy of Sciences, Institute of Vertebrate Paleontology and Paleoanthropology, Chinese Academy of Sciences, Beijing, 100044 China. E-mail: chenyue@ucas.ac.cn*

a Key Laboratory of Vertebrate Evolution and Human Origins of Chinese Academy of Sciences, Institute of Vertebrate Paleontology and Paleoanthropology, Chinese Academy of Sciences, Beijing, 100044, China

b Department of Scientific History and Archaeometry, University of Chinese Academy of Sciences, Beijing, 100049, China

Journal of RAMAN SPECTROSCOPY

Experimental details

Raman spectroscopy is believed to be a powerful tool for microstructure analysis of ancient artifacts because of its *in situ* detection, nondestructive process for sample measurement, rapid analysis, and unambiguous characterization and has been widely employed in studies of ceramic products,[12,13] glass materials,[14,15] and pigments.[16,17]

In the present study, Raman spectroscopy analyses were carried out on the surface of the red decoration shards directly after the alcohol rinsing. The Raman spectral signal was recorded by LabRam micro-spectrometer infinity (Horiba Jobin-Yvon, Longjumeau, France) at the 532 nm exciting radiation source whose power was kept low enough to avoid any sample damage. The Raman spectrometer resolution is about 1 cm^{-1}, and three spectra were selected for each sample. The wavenumber calibration of peak position was at 100 times magnification with a piece of crystal silicon. An Olympus BX41 confocal microscope was employed to focus the laser beam on red decorations at 50 times magnification. The segment baseline was subtracted by LABSPEC software, and the corrected Raman spectra were curve-fitted by Gaussian functions with the ORIGIN software, and more details could be found in the study of Robinet[14,18] and Colomban.[19,20]

The XRD pattern figure was obtained by Rigaku MiniFlex II Desktop X-ray diffractometer with Cu Kα radiation ($\lambda = 0.15406$ nm) on the powders scratched from the red decoration. As another aid, optical diffuse reflectance was measured directly on the red decoration surface using a VS-450 spectrophotometer with geometry of 45°/0° dual illumination, 45° gloss, in the spectral range of 400–700 nm. Spot size was set 6 mm, and standard illumination was chosen D65 with the standard view angle of 10°.

Results and discussion

Raman characterizations

According to previous researches, red over-glaze decoration of *Honglvcai* was ultrafine hematite particles suspending above the lead-base glass,[2,21] and its chemical composition had never changed before Qing dynasty (1636 AD).[22,23] From the Raman results of our samples (Fig. 1), it is indicated that red colorant in our samples is unambiguously hematite because all vibration wavenumber features are consistent with those recorded in previous literature.[24] The optical normal modes of hematite could be represented in D_{3d}^6 groups as $\Gamma = 2A_{1g} + 2A_{1u} + 3A_{2g} + 2A_{2u} + 5E_g + 4E_u$. Among these modes, six originate from IR-active vibrations ($2A_u + 4E_u$ modes), while another seven are from Raman-active vibrations ($2A_{1g} + 5E_g$ modes) whose wavenumbers are recorded as 225, 247, 293, 299, 412, 498, and 613 cm^{-1}.[24,25] All the seven typical modes are present in our samples as Fig. 1 shows.

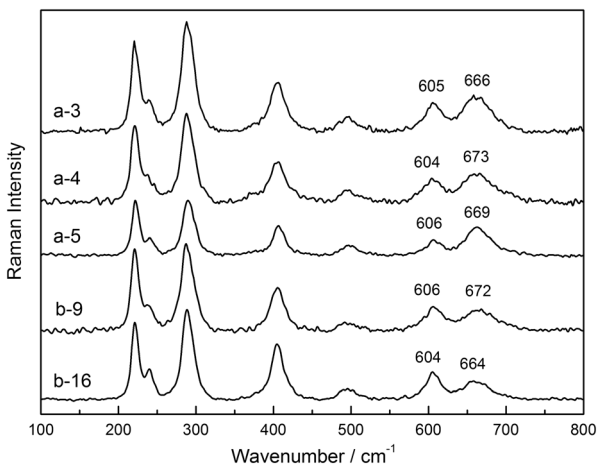

Figure 1. Raman spectra of samples of Linshui kiln.

Notably, the abnormal peak at the wavenumber of approximately 660 cm^{-1} with rather high intensity appears in the Raman spectra for all samples. Previous scholars noticed this anomalous peak although it was quite weak in their work, and explanations for this peak could be summarized as follows:

1) The superimposition effect of magnetite (Fe_3O_4) phase, where the most intense peak is around 660 cm^{-1}.[10,12]
2) The breakdown of hematite crystal lattice symmetry[25,26] caused by doped ions, thermal treatment, weathering, degradation, and so on. Consequently, the Raman peak at 660 cm^{-1} is excited by IR-active mode as the selection rules of Raman scattering changed.
3) The existence of nano-crystalline hematite that causes phonon confinement effect,[25,27] leading to the peak shift and broadening.

As to results in Fig. 1, the peak at 660 cm^{-1} for all samples displays much higher intensity than their peaks at about 610 cm^{-1}, which is different from previous studies in which the 660 cm^{-1} peaks are fairly weak. Magnetite is in the spinel structure with $Fd\bar{3}m$ space group, which has the Fe–O stretching mode corresponding to the peak in the wavenumber range between 550 (Fe^{2+}) and 725(Fe^{3+}) cm^{-1}.[28] Although magnetite is quite likely to exist, it makes few contributions to this extraordinary peak because other magnetite characteristic peaks[29,30] are not found in our spectra.[25] To acquire a further insight into the origin of this special peak, it is necessary to investigate the relationship between the Raman signal intensity of the peak at 610 cm^{-1} and the microstructure of hematite crystal. Consequently, full width at half maximum (FWHM) of 290 cm^{-1} is selected to reflect the long-range order condition of hematite crystal as it records the broadening of peak width, and the intensity of peak at 660 cm^{-1} is normalized by the peak intensity at 610 cm^{-1} in the form of intensity ratio (Fig. S3). It is found that the ratio of Raman intensity at 660–610 cm^{-1} increases as the FWHM of 290 cm^{-1} peak grows. The emergence of high intensity peak at 660 cm^{-1} relates to the breakdown of long-range order, which could originate from either the distortion of crystal lattice or decreasing of crystallite size, or the combination of these two effects.

X-ray diffraction patterns

In addition to the 660 cm^{-1} peak, there is a clear shift for 610 cm^{-1} peak towards low wavenumber at around 605 cm^{-1} (Fig. 1), which is obviously lower than the range 612–613 cm^{-1} reported in previous literature.[24] This shift is also unlikely to result from the existence of nano-scale crystal unless the crystalline size is below 8 nm.[31]

In the XRD pattern, the major phase is quartz, and most characteristic peaks of hematite also appear. This is reasonable because powders scratched from the decoration inevitably contain engobe, glaze, and/or even the body of porcelain. To estimate the hematite crystallite size roughly, powders of each sample

were scanned at lower speed about 0.5°/min in the range of 32–42° (Fig. 2). The broadening of the diffraction peaks at 33° is used based on Debye–Scherrer formula given as follows:

$$D = \frac{K\lambda}{w\cos\theta}$$

where D is the average diameter of crystallites, λ is the wavelength of radiation source (0.15406 nm in this work), θ is the angle of diffraction, w is the FWHM of the diffraction peak after broadening effect calibration of the instrument, and K is the constant whose value is often chosen as 0.9.[32–34] Calculation process was carried out by the software JADE 5.0, and crystallite sizes estimated are in the range of 26–40 nm (Table 1), which is far from tiny enough to cause obvious peak shift. In fact, the broadening of diffraction peak originates not only from the reduction of scale but also from the existence of strain inside the crystal lattice. On purpose of simplification, the latter effect is not considered in our calculation. Consequently, the crystal sizes estimated here should be smaller than their real values. Even in this case, the size is still much larger than 8 nm, thus implying that the main origin of 660 cm^{-1} peak in Raman spectra is the distortion of crystal structure instead of nanometer size effect.

Band gaps

Optical spectral reflectance (Fig. S4) is utilized to determine the band gap widths of hematite in our samples, and the equation used is given as follows:[35,36]

$$[F(R_\infty)h\nu]^2 = C(h\nu - Eg)$$

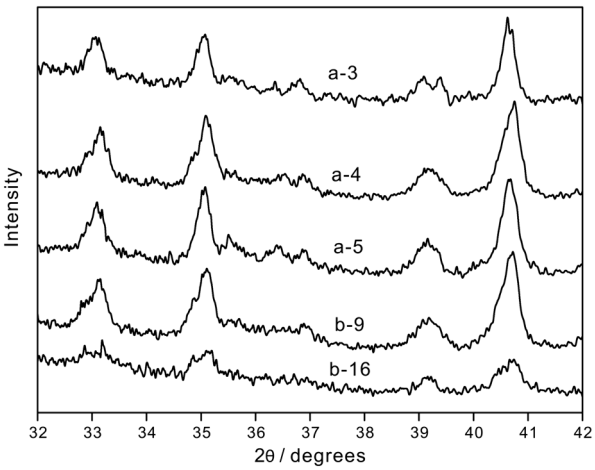

Figure 2. X-ray diffraction characterization of samples with the scan speed of 0.5°/min.

Table 1. X-ray diffraction peak widths and average estimated sizes of crystallites

Sample	FWHM (degrees)	2θ (degrees)	*D* (nm)
a-3	0.32	33.11	29
a-4	0.23	33.15	40
a-5	0.35	33.11	26
b-9	0.28	33.17	33
b-16	0.33	33.27	28

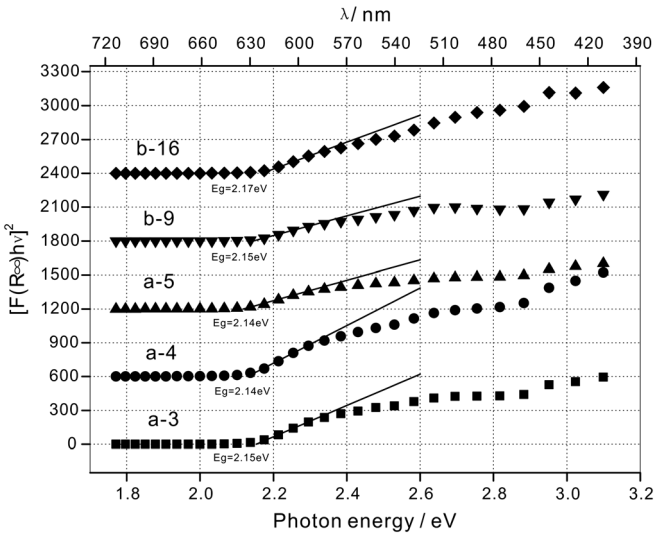

Figure 3. Plots of Kubelka–Munk transformed reflectance spectra of the samples.

where C is a proportionality constant, $h\nu$ is the photon energy, and E_g is the band gap width. R_∞ is the reflectance for an optically thick samples, measured at a specific wavelength, and $F(R_\infty)$ is Kubelka–Munk function defined by the equation:

$$F(R_\infty) = \frac{(1 - R_\infty)^2}{2R_\infty}$$

By previous literature, nano-sized hematite crystallites with the diameter around 8 nm also display the band gap of 2.2 eV,[37] while those with smaller sizes show higher band gap values in the range of 2.2–6.2 eV.[38] For our samples, all gaps estimated fall into the range of 2.14–2.16 eV (Fig. 3), which is consistent with those provided by previous researchers. In this work, existence of the tiny hematite crystallite with a diameter below 8 nm could not be absolutely excluded, but the major origin of 660 cm^{-1} peak in our spectra is crystal structure distortion. Substitution of metal impurities is inevitable because of the weathering effect from the burial environment. For hematite doped by ferrous or titanium ions, the intrinsic band gap is generally masked to be about 1.8 eV.[37] In M-doped (M = Al, In, or Y) hematite, there is broadening of the 225–290 cm^{-1} doublets and upshift especially for about 405 cm^{-1} as the Raman signature. In our results, effects of the metal impurity substitution are not so obvious as influences of manufacture.[28] As *Honglvcai* wares were produced after the two firing experiences: the first for the manufacture of white porcelain at high temperature and the second for the formation of over-glaze decoration at low temperature, it is thus assumed that the distortion mainly happened during the second firing process.

Conclusion

In the present study, red decorations on the glaze of *Honglvcai* shards excavated from Linshui kiln in Jin dynasty (1115–1234 AD) were analyzed by a series of scientific techniques. Further information of the colorant in the level of crystal size and band gap width was surveyed for the first time. Raman spectroscopy, X-ray diffractometry, and diffuse reflectance measurement were carried

Journal of RAMAN SPECTROSCOPY

out to acquire information on the identity, crystal size, and band gap width of the colorant. It was indicated that colorant of the red decorations is hematite crystallite whose average diameter is around 30 nm, and the crystal lattice structure was distorted perhaps because of thermal treatment during the second firing process at low temperature.

Acknowledgements

This study is financially supported by the Natural Science foundation of China (11275265) and the Knowledge Innovative Project of the Chinese Academy of Sciences and of the Graduate University Foundation. This work is also supported in part by the President Fund of UCAS and the China Postdoctoral Science Foundation (grant no. 2013M540130). The authors wish to thank the Chinese Academy of Cultural Heritage for the loan of the LabRam micro-spectrometer infinity.

References

[1] J. Li, History of History of Science and Technology in China, Ceramics Volume, Science Press, Beijing, **1998**.
[2] J. Jiang, *Nanfang Wenwu (Relics From South)* **2003**, *4*, 83.
[3] S. Wang, *Hebei Taoci (Hebei Ceramics)* **1986**, *2*, 37.
[4] The Chinese Ceramic Society, Chinese Ceramic History, Cultural Relics Press, Beijing, **1982**.
[5] C. Hu, Y. Chen, J. Zhu, L. Zhang, C. Wang, *Nanfang Wenwu (Relics From South)* **2012**, *2*, 174.
[6] Y. Xiong, W. He, *Wenwu Baohu yu Kaogu Kexue (Sciences of Conservation and Archaeology)* **2005**, *17*, 23.
[7] L. Cheng, M. Li, Y. Kim, C. Fan, S. Wang, Q. Pan, Z. Liu, R. Li, *Nucl. Instrum. Meth. Phys. Res. B* **2011**, *269*, 239.
[8] W. Zhao, G. Li, Z. Gao, B. Zhang, R. Li, X. Wu, G. Yao, X. Jia, S. Han, Z. Huang, *Chinese Sci. Bull.* **2000**, *45*, 663.
[9] R. Li, L. Yang, G. Li, W. Zhao, J. Xie, Z. Gao, B. Zhang, X. Sun, S. Feng, X. Jia, S. Han, Z. Huang, *Chinese Sci. Bull.* **2002**, *47*, 572.
[10] L. Wang, J. Zhu, Y. Yan, Y. Xie, C. Wang, *J. Raman Spectrosc.* **2009**, *40*, 998.
[11] L. Wang, H. Duan, J. Zhu, Y. Yan, Y. Xie, C. Wang, *Hejishu (Nuclear Techniques)* **2010**, *33*, 31.
[12] C. Lofrumento, A. Zoppi, E.M. Castellucci, *J. Raman Spectrosc.* **2004**, *35*, 650.
[13] J. Striova, C. Lofrumento, A. Zoppi, E.M. Castellucci, *J. Raman Spectrosc.* **2006**, *37*, 1139.
[14] L. Robinet, C. Coupry, K. Eremin, C. Hall, *J. Raman Spectrosc.* **2006**, *37*, 789.
[15] L.C. Prinsloo, J.C.A. Boeyens, M.M. van der Ryst, G Webb, *J. Mol. Struct.* **2012**, *1023*, 123.
[16] A. Hernanz, J M. Gavira-Vallejo, J.F. Ruiz-López, S. Martin, Ángel Maroto-Valiente, R. de Balbín-Behrmann, M. Menéndez, J.J. Alcolea-González, *J. Raman Spectrosc.* **2012**, *43*, 1644.
[17] I. Nastova, O. Grupče, B. Minčeva-Šukarova, S. Turan, M. Yaygingol, M. Ozcatal, V. Martinovska, Z. Jakovlevska-Spirovska, *J. Raman Spectrosc.* **2012**, *43*, 1729.
[18] L. Robinet, A. Bouquillon, J. Hartwig, *J. Raman Spectrosc.* **2008**, *39*, 618.
[19] P. Colomban, F. Treppoz, *J. Raman Spectrosc.* **2001**, *32*, 93.
[20] P. Colomban, H.D. Schreiber, *J. Raman Spectrosc.* **2005**, *36*, 884.
[21] F. Zhang, Z. Zhang, *Guisuanyan Xuebao (Journal of the Chinese Ceramic Society)* **1980**, *8*(4), 339.
[22] The Chinese Ceramic Society, Proceedings of Chinese Ancient Ceramics, Cultural Relics Press, Beijing, **1982**.
[23] G. Li, Y. Guo, Process Fundamentals of Chinese Famous Porcelain, Shanghai Science and Technology Press, Shanghai, **1988**.
[24] A. Zoppi, C. Lofrumento, E. M. Castellucci, Ph. Sciau, *J. Raman Spectrosc.* **2008**, *39*, 40.
[25] D. Bersani, P. P. Lottici, A. Montenero, *J. Raman Spectrosc.* **1999**, *30*, 355.
[26] A. M. Jubb, H. C. Allen, *ACS Appl. Mater. Inter.* **2010**, *2*, 2804.
[27] C. Baratto, P.P. Lottici, D. Bersani, G. Antonioli, G. Gnappi, A. Montenero, *J. Sol–gel Sci. Tech.* **1998**, *13*, 667.
[28] F. Froment, A. Tournié, P. Colomban, *J. Raman Spectrosc.* **2008**, *39*, 560.
[29] O. N. Shebanova, P. Lazor, *J. Solid State Chem.* **2003**, *174*, 424.
[30] O. N. Shebanova, P. Lazor, *J. Raman Spectrosc.* **2003**, *34*, 845.
[31] F.J. Owens, J. Orosz, *Solid State Commun.* **2006**, *138*, 95.
[32] J. Nanda, B.A. Kuruvilla, D.D. Sarma, *Phys. Rev. B* **1999**, *59*, 7473.
[33] J. Nanda, S. Sapra, D.D. Sarma, N. Chandrasekharan, G. Hodes, *Chem. Mater.* **2000**, *12*, 1018.
[34] H. Borchert, E.V. Shevchenko, A. Robert, I. Mekis, A. Kornowski, G. Grübel, H. Weller, *Langmuir* **2005**, *21*, 1931.
[35] A.E. Morales, E. Sánchez Mora, U. Pal, *Rev. Mex De Fís. S* **2007**, *53*, 18.
[36] B. Sun, J. Horvat, H.S. Kim, W. Kim, J. Ahn, G. Wang, *J. Phys. Chem. C* **2010**, *114*, 18753.
[37] B. Gilbert, C. Frandsen, E.R. Maxey, D.M. Sherman, *Phys. Rev. B* **2009**, *79*, 035108.
[38] M. Chirita, I. Grozescu, *Chem. Bull.* **2009**, *54*, 1.

Supporting information

Additional supporting information may be found in the online version of this article at the publisher's web site.

